Fission yeast TORC1 regulates phosphorylation of ribosomal S6 proteins in response to nutrients and its activity is inhibited by rapamycin

Akio Nakashima, Tatsuhiro Sato* and Fuyuhiko Tamanoi‡

Department of Microbiology, Immunology and Molecular Genetics, Molecular Biology Institute, Jonsson Comprehensive Cancer Center, University of California, Los Angeles, CA 90095-1489, USA

*Present address: Division of Biochemistry, School of Pharmaceutical Science, Kitasato University, 5-9-1 Shirokane, Minato-ku, Tokyo 108-8641, Japan

‡Author for correspondence (fuyut@microbio.ucla.edu)

Accepted 24 November 2009
Journal of Cell Science 123, 777-786

doi:10.1242/jcs.060319

Summary

Cellular activities are regulated by environmental stimuli through protein phosphorylation. Target of rapamycin (TOR), a serine/threonine kinase, plays pivotal roles in cell proliferation and cell growth in response to nutrient status. In *Schizosaccharomyces pombe*, TORC1, which contains Tor2, plays crucial roles in nutrient response. Here we find a nitrogen-regulated phosphoprotein, p27, in *S. pombe* using the phospho-Akt substrate antibody. Response of p27 phosphorylation to nitrogen availability is mediated by TORC1 and the TSC-Rhb1 signaling, but not by TORC2 or other nutrient stress-related pathways. Database and biochemical analyses indicate that p27 is identical to ribosomal protein S6 (Rps6). Ser235 and Ser236 in Rps6 are necessary for Rps6 phosphorylation by TORC1. These Rps6 phosphorylations are dispensable for cell viability. Rps6 phosphorylation by TORC1 also responds to availability of glucose and is inhibited by osmotic and oxidative stresses. Rapamycin inhibits the ability of TORC1 to phosphorylate Rps6, owing to interaction of the rapamycin-FKBP12 complex with the FRB domain in Tor2. Rapamycin also leads to a decrease in cell size in a TORC1-dependent manner. Our findings demonstrate that the nutrient-responsive and rapamycin-sensitive TORC1-S6 signaling exists in *S. pombe*, and that this pathway plays a role in cell size control.

Key words: Cell size, Nutrient response, Rapamycin, S6 phosphorylation, Signal transduction, TORC1

Introduction

Eukaryotic cells have evolutionarily conserved mechanisms by which protein-phosphorylation reactions mediate several cellular activities when cells perceive environmental stimuli such as growth factors, nutrients and stresses. Target of rapamycin (TOR), a serine/threonine kinase of the phosphatidylinositol kinase-related kinase family, plays central roles in controlling cell growth, cell-cycle progression and metabolism in response to environmental stimuli (reviewed by Chiang and Abraham, 2007; Wullschleger et al., 2006). In mammalian cells, TORC1 (mTORC1) contains mTOR, Raptor and mLST8, whereas mTORC2 consists of Rictor, mLST8 and mSIN1 in addition to mTOR. The immunosuppressant and anticancer drug rapamycin forms an intracellular complex with immunophilin FKBP12, thereby inhibiting preferentially TORC1 activity. Rapamycin-sensitive TORC1 signaling regulates temporal aspects of cell growth – protein synthesis, metabolism, transcription and autophagy – whereas rapamycin-insensitive TORC2 regulates spatial aspects of cell growth, such as organization of actin cytoskeleton (Wullschleger et al., 2006). mTORC1 is positively regulated by Rheb, a member of the Ras superfamily GTP-binding protein, and is negatively regulated by a tumor-suppressor protein complex consisting of tuberous sclerosis complex (TSC)1 and TSC2, which acts as a GTPase activating protein for Rheb. The TSC-Rheb-mTORC1 pathway regulates phosphorylation of ribosomal S6 kinases (S6K), members of the AGC (protein kinase A/protein kinase G/protein kinase C) kinase family and eIF4E-binding protein (4E-BP1) to promote protein synthesis (reviewed by Huang and Manning, 2008). Phosphorylation of S6K by mTORC1 leads to activation of S6K, which subsequently phosphorylates ribosomal protein S6, whereas phosphorylation of 4E-BP1 results in dissociation of 4E-BP1 from the initiation factor eIF4E, and it results in relieving the inhibition of the initiation factor (reviewed by Hay and Sonenberg, 2004). mTORC2 phosphorylates Akt/PKB, another member of the AGC kinase family, to activate its catalytic activity (Sarbassov et al., 2005).

Recently, the fission yeast *Schizosaccharomyces pombe* has emerged as an ideal system to study functions of TOR (reviewed by Aspuria et al., 2007; Otsubo and Yamamoto, 2008). Fission yeast has two *TOR* genes, *Tor1*$^{+}$ and *Tor2*$^{+}$. TORC1 contains Tor2, a Raptor homolog (Mip1) and an mLST8 homolog (Wat1; also known as Pop3), whereas TORC2 consists of Tor1, a Rictor homolog (Ste20), Sin1 and Wat1 (Alvarez and Moreno, 2006; Hayashi et al., 2007; Matsuo et al., 2007). Tor2 is a pivotal controller of the switch between cell cycle and cell differentiation by sensing nitrogen availability. Tor1 participates in leucine uptake, cell proliferation under stress conditions and sexual differentiation under nitrogen starvation (Alvarez and Moreno, 2006; Hayashi et al., 2007; Ikeda et al., 2008; Kawai et al., 2001; Matsuo et al., 2003; Matsuo et al., 2007; Uritani et al., 2006; Weisman and Choder, 2001; Weisman et al., 2005; Weisman et al., 2007). In addition to the TOR complexes, fission yeast has homologous genes of mammalian *TSC1* and *TSC2* (*tsc1*$^{+}$ and *tsc2*$^{+}$, respectively), and a Rheb homolog (*rhb1*$^{+}$). The products of these genes are involved in vegetative growth, amino acid uptake and nitrogen starvation response (Aspuria and Tamanoi, 2008; Mach et al., 2000; Matsumoto et al., 2002; Nakase et al., 2006; Tabancay et al., 2003; Urano et al., 2005; van

Slegtenhorst et al., 2004; Yang et al., 2001). Rhb1 interacts with Tor2 (Urano et al., 2005; Uritani et al., 2006).

Several genetic analyses between TSC-Rhb1 and TORC1 have shown that the TSC-Rhb1 pathway regulates TORC1 activity (Matsuo et al., 2007; Urano et al., 2007; Uritani et al., 2006; Weisman et al., 2007). By contrast, no downstream effectors of TORC1 have been identified. Here we screened for nitrogen-regulated phosphoproteins in fission yeast using the anti-phospho-Akt substrate (PAS) antibody and found four phosphoproteins. One of them, p27, was further characterized, and our findings showed that p27 phosphorylation is regulated by the TORC1 signaling in response to nutrient conditions and several stresses. p27 was identified as a ribosomal protein S6 (Rps6) by bioinformatic and biochemical analyses. In addition, we demonstrated that rapamycin inhibits phosphorylation of Rps6 by TORC1 and reduces cell size in a Tor2-dependent manner.

Results

Phosphorylation of p27 recognized by anti-PAS antibody responds to nitrogen availability

The phosphorylation-site-specific antibody anti-PAS was originally designed against the Akt consensus phosphorylation motif Arg-Xaa-Arg-Xaa-Xaa-[Ser(*P*)/Thr(*P*)], where Xaa represents any amino acid, and Ser(*P*) or Thr(*P*) is phosphorylated serine or threonine, respectively. The anti-PAS antibody has been used to screen for growth-factor-regulated and nutrient-regulated phosphoproteins, which include not only the actual substrates of Akt but also substrates of S6K and AMP-activated protein kinase in mammalian cells (Eguchi et al., 2009; Kane et al., 2002; Manning et al., 2002; Miyamoto et al., 2008). To examine nitrogen-regulated phosphoproteins by using the anti-PAS antibody, fission yeast cells were cultured in medium in the presence or absence of ammonium as the sole nitrogen source. The cell extracts were subjected to SDS-PAGE and immunoblotting with the anti-PAS antibody (Fig. 1A). An intense band of approximate 27-kDa protein, which is designated as p27, was detected when the cells were incubated in a nitrogen-rich medium, but the p27 protein was not detected 15 minutes after the shift to nitrogen-starvation conditions. Furthermore, three other distinct proteins designated as p150, p90 and p70 were observed in nitrogen-rich conditions, and the intensity of these bands was significantly decreased 30 minutes after the shift to nitrogen starvation (Fig. 1A). It has been known that nutrient limitation induces the phosphorylation of the α-subunit of eukaryotic initiation factor 2α (eIF2α) at Ser52 in a Gcn2-dependent manner (Zhan et al., 2004). Similarly, nitrogen depletion led to the induction of phosphorylation of Ser52 in eIF2α (Fig. 1A).

In this study, we focused on the characterization of p27. The band of p27 was not detected following phosphatase treatment, suggesting that the band of p27 recognized by the anti-PAS antibody under nitrogen-rich conditions actually results from the phosphorylation of p27 (Fig. 1C). Fig. 1B shows that re-addition of ammonium to cells starved for nitrogen source rapidly induced p27 phosphorylation, with the maximal level reached by 20 minutes (Fig. 1B). Taken together, these results suggest that p27 phosphorylation recognized by the anti-PAS antibody is regulated in response to nitrogen availability.

TORC1, but not the SAPK, cAMP-PKA or TORC2 pathways, regulates phosphorylation of p27 in response to nitrogen availability

Recent studies in fission yeast have demonstrated that Tor2 and Tor1, which constitute TORC1 and TORC2, respectively, have been implicated in cellular responses to nitrogen availability (Aspuria et al., 2007; Otsubo and Yamamoto, 2008). Thus, we investigated whether the function of Tor2 and/or Tor1 is involved in the regulation of p27 phosphorylation in response to nitrogen status. To address this issue, we first utilized two mutants, *tor2*^{L1310P} and *tor2*^{E2221K}, which carry activating mutations in *tor2*$^{+}$ gene on its chromosomal locus. These two mutants confer Rhb1-independent cell proliferation in nutrient-rich conditions and show delayed G1 arrest and decreased sporulation efficiency under nutrient starvation (Urano et al., 2007). In both active mutants, phosphorylation of p27 was maintained at a high level even under nitrogen starvation compared with that in the wild-type cells (Fig. 2A). Indeed, activity of the Tor2^{E2221K} mutant was higher than that of the wild-type Tor2 in the in vitro kinase assay using 4E-BP1 as a substrate (supplementary material Fig. S1). Phosphorylation of p27 in the *tor2*^{L1310P} cells was still observed by 30 minutes after the shift to nitrogen depletion, but diminished by 60 minutes (Fig. 2B). By contrast, phosphorylation of eIF2α at Ser52 was increased in the wild-type cells and the active mutants under nitrogen starvation (Fig. 2A), suggesting that the modulation of the Gcn2-eIF2α pathway in response to nitrogen availability is independent of Tor2 activity. We next examined p27 phosphorylation in two distinct temperature-sensitive *tor2* mutants: *tor2-ts6* and *tor2-ts10*. These mutants arrest cell cycle in G1 phase and initiate sexual development, mimicking nitrogen starvation at the non-permissive temperature even in nitrogen-rich conditions (Matsuo et al., 2007). In both *tor2-ts* mutants, increase in p27 phosphorylation by the re-addition of ammonium after nitrogen starvation was markedly suppressed at the non-permissive temperature (34°C) compared with

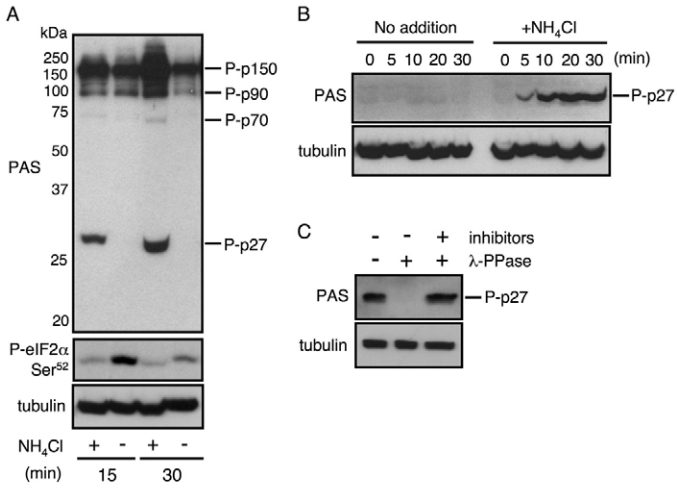

Fig. 1. Phosphorylation of p27 in response to nitrogen availability is recognized by the anti-PAS antibody. (**A**) Cells of JUp1204 were cultured in EMM medium at 30°C to exponential phase, then washed and incubated in EMM with (+) or without (–) ammonium for the indicated time points. Cell extracts were probed with anti-PAS antibody or with anti-phospho-eIF2α (Ser51) antibody to detect phosphorylation of eIF2α at Ser52. In the top panel, positions of predicted phosphoproteins (p27, p70, p90 and p150) and molecular size markers are indicated. Tubulin is shown as a loading control (bottom). (**B**) Exponentially growing cells of JUp1204 were starved in EMM-N (a nitrogen-free version of EMM) for 1 hour, and then water (no addition) or 0.5% ammonium chloride (final concentration) was added. The cells were taken at the indicated time points, and extracts were probed with the anti-PAS antibody for phosphorylation of p27 or anti-tubulin antibody. (**C**) Extracts from exponentially growing cells of JUp1204 were treated with λ-phosphatase in the presence or absence of its inhibitors and probed for phosphorylation of p27 or tubulin.

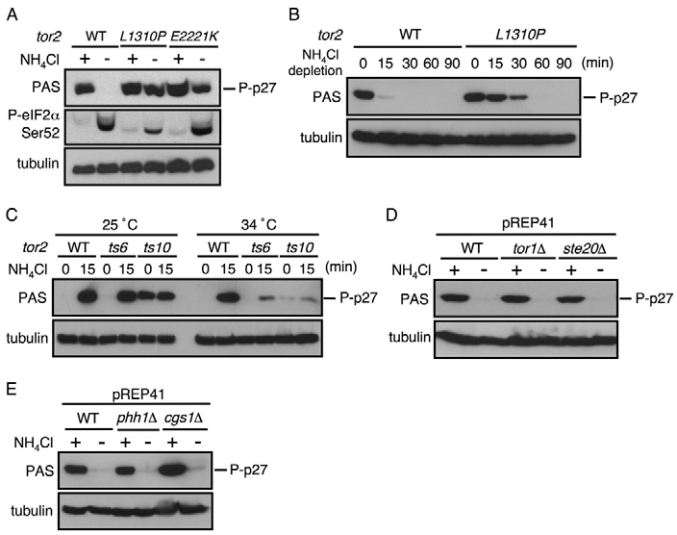

Fig. 2. TORC1 regulates p27 phosphorylation. Extracts were subjected to immunoblotting with the indicated antibodies. (**A**) Cells of JUp1348 (WT), JUp1350 (*tor2*^{L1310P}) and JUp1352 (*tor2*^{E2221K}) were grown in EMM at 30°C to exponential phase, then washed and treated with EMM with (+) or without (–) ammonium for 15 minutes. (**B**) Exponentially growing cells of JUp1348 (WT) and JUp1350 (*tor2*^{L1310P}) (0 minutes) were washed and incubated in EMM-N (a nitrogen-free version of EMM). The cells were harvested for the indicated time points. (**C**) Cells of JUp1246 (WT), JUp1247 (*tor2-ts6*) and JUp1252 (*tor2-ts10*) were grown in EMM at 25°C to exponential phase. When cells were treated at a non-permissive temperature, cell culture was shifted to 34°C for 1 hour before the cells were transferred to pre-warmed EMM-N. After incubation in EMM-N for 1 hour at either 25°C or 34°C, the cells were added with ammonium or water and then incubated for 15 minutes. (**D**) Exponentially growing cells of JY450 (WT), TA99 (*tor1*Δ) and JT293 (*ste20*Δ) carrying pREP41 (vector) in EMM+Adenine were treated with EMM+Adenine (+) or EMM-N (–) for 15 minutes at 30°C. (**E**) JY450 (WT), FY13927 (*phh1*Δ) and JZ858 (*cgs1*Δ) carrying pREP41 (vector) were grown and treated as described in D.

that in the wild type, whereas the increase in protein phosphorylation by the addition of ammonium in the *tor2-ts6* mutant at the permissive temperature (25°C) was comparable to that in the wild type (Fig. 2C). Consistent with findings from previous studies, activity of *tor2-ts10* was less than that of *tor2-ts6* in nitrogen-rich conditions at the permissive temperature (Matsuo et al., 2007). At the permissive temperature, p27 phosphorylation was maintained in the *tor2-ts10* mutant under nitrogen-depletion conditions (Fig. 2C). Taken together, these results indicate that TORC1 including Tor2 plays a crucial role in the regulation of p27 phosphorylation in response to nitrogen status, namely that the level of p27 phosphorylation reflects TORC1 activity.

Disruption of *tor1*$^{+}$ or *ste20*$^{+}$ causes defects in cellular responses to nitrogen starvation, including cell-cycle arrest in G1 phase and entry into sexual-differentiation process, suggesting that these two TORC2 components also participate in nitrogen-starvation responses (Alvarez and Moreno, 2006; Hayashi et al., 2007; Hilti et al., 1999; Ikeda et al., 2008; Kawai et al., 2001; Matsuo et al., 2007; Weisman and Choder, 2001). We assessed phosphorylation of p27 in *tor1*Δ and *ste20*Δ cells to clarify the role of TORC2 in the regulation of this protein phosphorylation. During our investigation, we noted that downregulation of p27 phosphorylation by nitrogen starvation was attenuated in cells possessing a leucine auxotrophy (denoted as *leu1*$^{-}$ or *ade6*$^{-}$*leu1*$^{-}$) (supplementary material Fig. S2). It is possible that cells uptake a large amount of leucine before nitrogen starvation owing to its leucine auxotrophy. Intracellular leucine might keep TORC1 activity even under starvation conditions, because leucine is important for TORC1 activity in mammalian cells (Hidayat et al., 2003). Thus, the strains carrying the leucine auxotrophy used in this study were transformed with a plasmid having a leucine marker. As shown in Fig. 2D, the response of p27 phosphorylation in the *tor1*Δ or *ste20*Δ cells to nitrogen availability was comparable to that in the wild-type strain. These results suggest that TORC2 is not implicated in the regulation of p27 phosphorylation.

The stress-activated protein kinases (SAPKs) and cyclic AMP (cAMP)-dependent protein kinase (PKA) pathways are also involved in cellular responses to nitrogen starvation. Disruption of *phh1*$^{+}$, which is also known as *sty1*$^{+}$ and *spc1*$^{+}$ and encodes a SAPK, interferes with cell-cycle arrest in G1 and sexual differentiation in response to nitrogen starvation (Kato et al., 1996; Shiozaki and Russell, 1996; Wilkinson et al., 1996). However, null mutation of *cgs1*$^{+}$, which encodes the regulatory subunit of PKA, leads to constitutive activation of PKA and prevents sexual differentiation in response to nitrogen starvation (Kunitomo et al., 2000). We therefore examined the role of the SAPKs and PKA pathways in the regulation of p27 phosphorylation. Similar to the wild type, phosphorylation of p27 in *phh1*Δ and *cgs1*Δ cells was decreased in response to nitrogen depletion (Fig. 2E). These results suggest that downregulation of p27 phosphorylation after the shift to nitrogen starvation is independent of the SAPKs and PKA pathways.

The TSC1-TSC2 complex and Rhb1 are involved in the regulation of p27 phosphorylation

In mammalian cells, loss of either of the *TSC* genes or overexpression of Rheb suppresses, at least in part, downregulation of the mTORC1 activity under nutrient starvation (Gao et al., 2002; Garami et al., 2003; Inoki et al., 2002; Tee et al., 2003). Several lines of evidence from genetic studies in fission yeast have demonstrated that the TSC1-TSC2 complex negatively regulates TORC1, and conversely, Rhb1, a Rheb homolog, activates TORC1 activity (Aspuria et al., 2007; Otsubo and Yamamoto, 2008). Thus, we evaluated p27 phosphorylation in *tsc2*Δ cells to test the role of the TSC1-TSC2 complex in the TORC1-mediated p27 phosphorylation. Although phosphorylation of p27 in *tsc2*Δ cells was decreased under nitrogen starvation, the phosphorylation under the starvation was still maintained at roughly half level compared with that under nitrogen-rich conditions (Fig. 3A). This persistence of p27 phosphorylation in *tsc2*Δ cells was detected by 30 minutes after the shift to a nitrogen-depletion condition (Fig. 3B), suggesting that the disruption of *tsc2*$^{+}$ results in partial activation of TORC1 under nitrogen depletion. To investigate the effect of Rhb1 activity on p27 phosphorylation, we next employed the cells expressing two myc-tagged *rhb1* mutants, *rhb1*^{V17A} and *rhb1*^{K120R}, which have been identified as hyperactivating mutations in fission yeast (Murai et al., 2009; Urano et al., 2005), from the chromosomal *rhb1*$^{+}$ locus. Phosphorylation of p27 in *rhb1*^{V17A} but not in the wild-type *rhb1*$^{+}$ or *rhb1*^{K120R} was significantly resistant to nitrogen starvation, similar to that in *tsc2*Δ cells (Fig. 3C). p27 phosphorylation in *rhb1*^{V17A} persisted 30 minutes after the shift to nitrogen depletion (Fig. 3D). Furthermore, overexpression of *rhb1*^{K120R} and *rhb1*^{N153T}, another hyperactivating mutation, in the wild-type cells caused resistance to p27 phosphorylation decrease by nitrogen starvation (supplementary material Fig. S3), suggesting that activating mutations of *rhb1* also lead to partial activation of TORC1 under

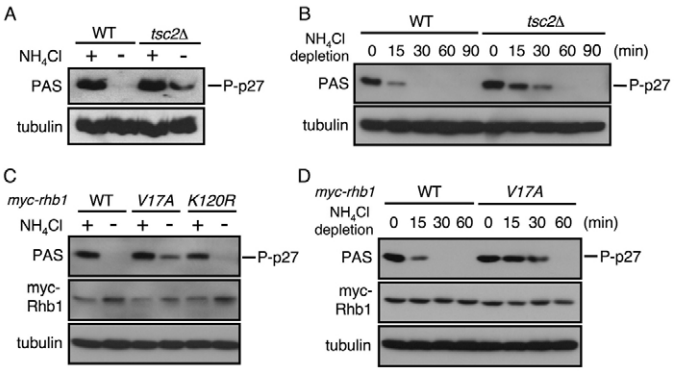

Fig. 3. The Tsc1-Tsc2 complex and Rhb1 are involved in the regulation of p27 phosphorylation. Extracts were subjected to immunoblotting with the indicated antibodies. (**A**) JUp1204 (WT) and PJ001 (*tsc2*Δ) were grown and treated as described in Fig. 2A. (**B**) Cells of 972 (WT) and PJ001 (*tsc2*Δ) were treated with EMM-N (a nitrogen-free version of EMM) as described in Fig. 2B. (**C**) JUp1188 (WT), JUp1190 (*rhb1*^{V17A}) and JUp1194 (*rhb1*^{K120R}) were grown and treated as described in Fig. 2A. The amount of myc-Rhb1 was examined by anti-myc antibody. (**D**) JUp1188 (WT) and JUp1190 (*rhb1*^{V17A}) were treated with EMM-N as described in Fig. 2B.

nitrogen starvation. Mutation of Ser16 to His in human Rheb causes a hyperactivation of the mTORC1 pathway (Yan et al., 2006). In fission yeast, overexpression of wild-type *rhb1*$^{+}$ and *rhb1*^{S16H} did not activate TORC1 activity in p27 phosphorylation (supplementary material Fig. S3). There seems to be a difference in the strength of Rhb1 mutants. These results suggest that the TSC1-TSC2 complex negatively regulates the TORC1 pathway, whereas Rhb1 activates TORC1 activity.

Identification of ribosomal protein S6 as a TORC1-regulated phosphoprotein, p27

The anti-PAS antibody used in this study mainly recognizes the consensus phosphorylation motif, [Arg/Lys]-Xaa-[Arg/Lys]-Xaa-Xaa-[Ser(*P*)/Thr(*P*)]. We next used the Scansite program (http://scansite.mit.edu) (Yaffe et al., 2001) to identify candidates for p27, which are predicted to have the sites [Arg/Lys]-Xaa-[Arg/Lys]-Xaa-Xaa-[Ser(*P*)/Thr(*P*)]. The most likely candidates found in the *S. pombe* SWISS-PROT database in the 26- 28-kDa molecular-weight range are listed in Table 1. Because p27 phosphorylation was regulated by the TORC1 pathway in response to nitrogen availability as described above, we focused on two ribosomal protein (rp) S6s, Rps601 and Rps602, among all the candidates. In the mammalian system, mTORC1 regulates rpS6 phosphorylation by activation of S6K. S6K can phosphorylate the Akt consensus phosphorylation motif (reviewed by Ruvinsky and Meyuhas, 2006). In fact, the anti-PAS antibody recognizes the mTORC1-S6K-dependent phosphorylation of S6 (Kane et al., 2002; Manning et al., 2002). Both Rps6 proteins in fission yeast show high homology with those in human and budding yeast. Moreover, residues adjacent to S6K-phosphorylation sites Ser235 and Ser236 in human rpS6 are highly conserved in fission yeast and budding yeast Rps6 (supplementary material Fig. S4) (Ruvinsky and Meyuhas, 2006). In addition, Ser235 in both of the fission yeast Rps6 proteins is consistent with the phosphorylated serine residue within the consensus phosphorylation motif recognized by the anti-PAS antibody.

To determine whether p27 is identical to Rps6, we first constructed null mutants of either *rps601*$^{+}$ or *rps602*$^{+}$ and assessed the phosphorylation level of p27 in those mutants. We were unable to obtain a double disruptant of *rps601*$^{+}$ and *rps602*$^{+}$ in approximately 8×10^{5} spores from heterozygous diploid cells, thus the double disruption is probably lethal (data not shown). Level of p27

Table 1. Candidates for p27

Gene identifier	Gene symbol	Predicted mass (kDa)	Description
SPAC13D6.05	*alp11*	26.6	Cell-polarity protein
SPAC27D7.12c	*but1*	27.4	Uba3-binding protein
SPAC4G9.11c	*cmb1*	26.3	Mismatch-binding protein
SPAC31G5.16c	*dpm1*	26.6	Dolichol-phosphate mannosyltransferase catalytic subunit
SPAC17A5.13		26.4	GTP cyclohydrolase I
SPAPB24D3.04c	*mag1*	26.3	DNA-3-methyladenine glycosylase 1
SPAC10F6.12c	*mam4*	26.5	Protein-S-isoprenylcysteine O-methyltransferase
SPBC11G11.03		26.6	mRNA turnover protein 4 homolog
SPAC1F7.13c	*rpl801*	27.1	60S ribosomal protein L2
SPAC3A12.04c		26.7	Probable ribonuclease P protein subunit 3
SPAC3G9.10c	*ski6*	26.8	Putative exosome complex exonuclease RRP41
SPBC16G5.14c	*rps3*	27.5	40S ribosomal protein S3
SPAC13G6.07c	*rps601*	27.4	40S ribosomal protein S6-A
SPAPB1E7.12	*rps602*	27.4	40S ribosomal protein S6-B
SPAC13G6.05c		27.5	Hypothetical protein
SPAC22G7.03		26.8	Hypothetical protein
SPAC15F9.01c		26.2	Hypothetical protein
SPAC1D4.09c		27.0	Hypothetical protein
SPBC582.09	*pex11*	26.4	Peroxisomal biogenesis factor 11
SPBC651.04		27.2	Hypothetical protein
SPAC15A10.05c	*mug182*	26.4	YjeF family protein
SPAC4C5.01		27.3	Haloacid dehalogenase-like hydrolase
SPAC17H9.03c	*rdl1*	26.0	RAD51D-like protein 1
SPAC23H3.12c		26.1	Hypothetical protein
SPAC22H12.01c	*mug35*	27.5	Hypothetical protein
SPBP23A10.12		27.6	FRG1 family protein
SPBC839.14c		27.0	Methyltransferase (predicted)
SPBC1921.07c	*sgf29*	27.5	SAGA complex subunit (predicted)
SPCC297.06c		27.6	Hypothetical protein

phosphorylation in the *rps602*Δ mutant cells was significantly decreased compared with that in the wild-type cells in the presence of ammonium (Fig. 4A) and, in the *rps601*Δ cells, the phosphorylation was slightly decreased. We next replaced chromosomal *rps602*$^{+}$ with a *myc-rps602* allele, which expresses an N-terminal tagged myc-Rps602 under the control of the endogenous *rps602* promoter, in an *rps601*Δ background. The *rps601*Δ*myc-rps602* cells grew similarly to the *rps601*Δ cells; therefore, the myc epitope did not interfere with the function of the ribosomal protein. In the *rps601*Δ*myc-rps602* cells, only phosphorylation of myc-Rps602, of which the molecular weight is increased by the addition of the myc tag compared with that of p27, was observed under nitrogen-rich conditions (Fig. 4B). This suggests that phosphorylation of p27 is substituted by that of myc-Rps602 in *rps601*Δ*myc-rps602*. Nitrogen depletion abolished the phosphorylation of the tagged protein (Fig. 4B). In Fig. 4C, myc-Rps601 or -Rps602 was expressed from the *nmt1*$^{+}$ promoter in pREP1 vector and immunoprecipitated with anti-myc antibody. The immunoprecipitated myc-Rps6 proteins were examined for phosphorylation using the anti-PAS antibody. As can be seen, the immunoprecipitated myc-Rps601 and -Rps602 were phosphorylated, whereas phosphorylation of the immunoprecipitates from nitrogen-starved cells was not observed. Taken together, p27 is identical to the two Rps6 proteins, and phosphorylation of Rps6 is modulated by the TORC1 pathway in response to nitrogen availability.

In previous reports, expression of *rps6*$^{+}$ mRNA is greatly reduced by nitrogen depletion (Bonnet et al., 2000; Nakashima et al., 2002). We examined the effects of nitrogen depletion on protein level of Rps602 in the *rps601*Δ*myc-rps602* strain. As shown in Fig. 4D (left), the protein level of myc-Rps602, which was expressed under the control of its own promoter as mentioned above, did not change for at least 90 minutes under nitrogen depletion, although phosphorylation of myc-Rps602 was abolished. These findings suggest that the decrease in Rps6 phosphorylation under nitrogen starvation is not caused by a decrease in the amount of protein.

Ser235 and Ser236 of Rps6 are crucial for its phosphorylation

To investigate whether the conserved Ser235 and Ser236 residues in Rps6 are important for the phosphorylation of Rps6, we constructed a series of mutations in both *rps6*$^{+}$ genes, in which either or both the serine residues were replaced by alanine. These mutants tagged with the myc epitope at their N-termini were expressed under the control of the *nmt1*$^{+}$ promoter in pREP1 in an *rps602*Δ background. Because the *rps601*$^{+}$ gene exists, the band of endogenous Rps601 phosphorylation was observed below that of myc-Rps6 in immunoblotting with the anti-PAS antibody (top panels in Fig. 5A,B). Unlike wild type, both myc-Rps601^{S235A,S236A} and -Rps602^{S235A,S236A} failed to be phosphorylated even in the presence of ammonium (Fig. 5A). Furthermore, as shown in Fig. 5B, phosphorylation of myc-Rps601^{S235A} and -Rps602^{S235A} under nitrogen-rich conditions was markedly diminished, and the phosphorylation of myc-Rps601^{S236A} and -Rps602^{S236A} was hardly detected. These results suggest that both Ser235 and Ser236 in Rps6 play a key role in phosphorylation of this ribosomal protein in nitrogen-rich conditions and that the TORC1 pathway would regulate phosphorylation of Rps6 at Ser235 and Ser236. To further examine the biological role of phosphorylations of Ser235 and Ser236 in Rps6, we replaced both the serine residues of the chromosomal *rps602* gene by alanine in an *rps601*Δ background. Whereas the

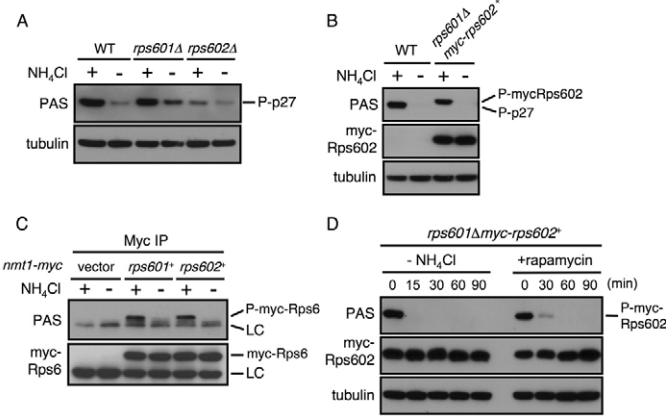

Fig. 4. Identification of ribosomal protein S6 as p27. (**A**,**B**,**D**) Extracts were subjected to immunoblotting with the indicated antibodies. (**A**) Cells of 972 (WT), AN0094 (*rps601*Δ) and AN0097 (*rps602*Δ) were grown and treated as described in Fig. 2A. (**B**) JUp1204 (WT) and AN0138 (*rps601*Δ *myc-rps602*$^{+}$) were grown and treated as described in Fig. 2A. The amount of myc-Rps602 was examined by anti-myc antibody. (**C**) AN0098 (*rps602*Δ) was transformed with pREP1-myc (vector), pREP1-myc-*rps601*$^{+}$(*rps601*$^{+}$) or pREP1-myc-*rps602*$^{+}$(*rps602*$^{+}$), and the transformants were treated as described in Fig. 2A. The immunoprecipitates with anti-myc antibody were subjected to immunoblotting with the indicated antibodies. LC denotes light chain of immunoglobulin caused by immunoprecipitation. (**D**) AN0138 (*rps601*Δ *myc-rps602*$^{+}$) (0 minutes) was transferred to EMM-N or added with 200 μM rapamycin (final concentration). The cells were incubated for the indicated time.

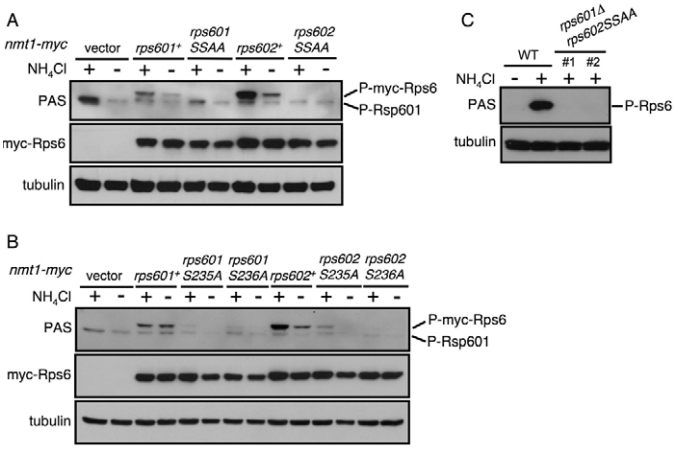

Fig. 5. Identification of phosphorylation sites in Rps6. Extracts were subjected to immunoblotting with the indicated antibodies. (**A**) Ser235 and Ser236 in Rps6 are necessary for phosphorylation of the ribosomal protein. AN0098 (*rps602*Δ) cells harboring pREP1-*myc* (vector), pREP1-*myc-rps601*$^{+}$ (*rps601*$^{+}$), pREP1-*myc-rps601*^{S235A,S236A} (*rps601SSAA*), pREP1-*myc-rps602*$^{+}$ (*rps602*$^{+}$) or pREP1-*myc-rps602*^{S235A,S236A} (*rps602SSAA*) were treated as described in Fig. 2A. (**B**) AN0098 (*rps602*Δ) cells harboring pREP1-*myc* (vector), pREP1-*myc-rps601*$^{+}$ (*rps601*$^{+}$), pREP1-*myc-rps601*^{S235A} (*rps601S235A*), pREP1-*myc-rps601*^{S236A} (*rps601S236A*), pREP1-myc-*rps602*$^{+}$ (*rps602*$^{+}$), pREP1-*myc-rps602*^{S235A} (*rps602S235A*) or pREP1-myc-*rps602*^{S236A} (*rps602S236A*) were treated as described in Fig. 2A. (**C**) Cells of 972 (WT), AN0228 (*rps601*Δ *rps602SSAA*; #1) and AN0229 (*rps601*Δ*rps602SSAA*; #2) were grown in YES at 30°C to exponential phase and harvested as +N (+). A half volume of 972 was washed and treated with EMM-N (a nitrogen-free version of EMM; –) for 30 minutes.

rps601Δrps602^{S235A,S236A} mutant (*rps601Δrps602SSAA*) did not exhibit phosphorylation of Rps6 (Fig. 5C), the mutant cells grew similarly to the *rps601Δ* cells (data not shown), suggesting that phosphorylation of Ser235 and Ser236 in Rps6 is dispensable for viability. In addition, there was little difference in response of the *rps601Δrps602SSDD* mutant, which is a phosphorylation-mimicking mutants, to nitrogen starvation compared with that of the wild-type cell (data not shown).

Characterizations of regulation of Rps6 phosphorylation

The above studies establish that the phosphorylation of Rsp6 can be used to monitor effects of a variety of conditions on TORC1 signaling. We have examined a number of conditions that might influence TORC1. In mammalian cells, glucose depletion, which induces low energy status in the cells, causes downregulation of mTOR activity through the activation of AMP-activated protein kinase (AMPK), an energy sensor (reviewed by Kimball, 2006). We first tested the effect of glucose starvation on TORC1 activity. Glucose starvation (0.1% glucose and 3% glycerol as carbon sources) quickly reduced phosphorylation of Rps6 in the wild-type cells similar to what was observed following nitrogen starvation, whereas downregulation of the protein phosphorylation by glucose starvation was partially attenuated by a *tor2* activating mutation (*tor2*^{L1310P}) (Fig. 6A). However, this resistance to glucose depletion in *tor2*^{L1310} was somewhat weak compared with that after nitrogen depletion in the *tor2* active mutant. The amount of myc-Rps602 in *rps601Δ myc-rps602* cells was not altered during glucose depletion (data not shown). Taken together, TORC1 activity is regulated by both nitrogen and glucose availability.

In mammalian cells and budding yeast, TORC1 activity is inhibited by several kinds of stress, including oxidative and osmotic stresses (Patel et al., 2002; Urban et al., 2007). Therefore, we investigated the effect of oxidative and osmotic stresses on TORC1 activity. Phosphorylation of Rps6 in wild-type cells was abolished completely by 60 minutes after the addition of H_2O_2, whereas that in the *tor2* active mutant (*tor2*^{L1310P}) was unaltered (Fig. 6B). In addition, high osmotic stress abolished phosphorylation of Rps6 in wild-type cells by 60 minutes (Fig. 6C). In contrast to H_2O_2, Rps6 phosphorylation in *tor2*^{L1310P} was abolished by 60 minutes after the shift to high osmotic medium (Fig. 6C). When *rps601Δ myc-rps602* cells were subjected to either oxidative or osmotic stress, the amount of the chromosomally expressed myc-Rps602 was unaltered (data not shown). These results suggest that TORC1 activity is inhibited by oxidative and osmotic stresses, although the inhibition of TORC1 activity by these stresses is slower than the inhibition by nutrient starvation.

Rapamycin inhibits Rps6 phosphorylation in an Fkh1-Tor2-dependent manner

In mammalian cells and budding yeast, rapamycin inhibits TORC1 activity when the drug-FKBP12 complex interacts with the FRB domain in TOR (Chen et al., 1995; Lorenz and Heitman, 1995). Examination of Rps6 phosphorylation provides a convenient assay to examine whether rapamycin inhibits TORC1 function in fission yeast. As shown in Fig. 7A, phosphorylation of Rps6 was markedly diminished by 30 minutes after the addition of rapamycin and was not detected by 60 minutes. Fig. 4D shows that the phosphorylation of myc-Rps602 in *rps601Δ myc-rps602* was abolished by 60 minutes after the addition of rapamycin. The amount of the tagged protein was unaffected for at least 90 minutes after the addition of the drug. We also found that 200 nM rapamycin is required to abolish Rps6 phosphorylation (Fig. 7B). In budding yeast, rapamycin as well as nitrogen starvation induces phosphorylation of Ser52 in eIF2α (Cherkasova and Hinnebusch, 2003; Kubota et al., 2003). In fission yeast, phosphorylation of Ser52 in eIF2α exhibited no increase during the rapamycin treatment (Fig. 7A) (Petersen and Nurse, 2007), suggesting that rapamycin does not affect eIF2α phosphorylation.

To further determine whether the decline in Rps6 phosphorylation by rapamycin is due to inhibition of Tor2 activity by the drug, we employed two distinct mutants, *fkh1Δ*, which is a null mutant of FKBP12, and *tor2*^{S1837E}, in which chromosomal wild-type *tor2*$^{+}$ was replaced with the *tor2*^{S1837E} mutation. The latter mutant has a mutation of the conserved serine residue in the FRB domain; this residue is crucial for the binding between the FRB domain in TOR and the FKBP12-rapamycin complex in other eukaryotes (Chen et al., 1995; Helliwell et al., 1994; Lorenz and Heitman, 1995; Stan et al., 1994). In fission yeast, a mutation of Ser1834 to Glu in Tor1

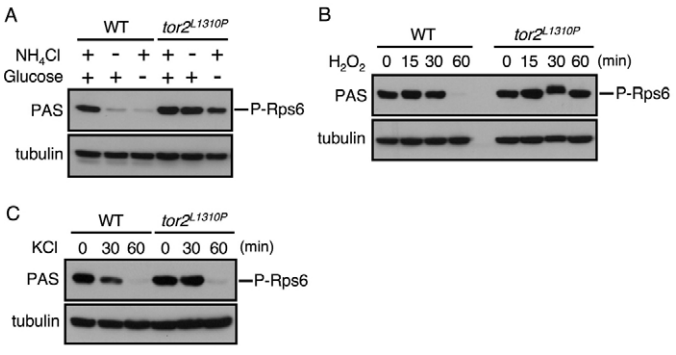

Fig. 6. Characterization of the TORC1-dependent Rps6 phosphorylation. Extracts were subjected to immunoblotting with the indicated antibodies. (**A**) TORC1 activity is diminished by glucose depletion. JUp1204 (WT) and JUp1350 (*tor2*^{L1310}) were treated with EMM, EMM-N (a nitrogen-free version of EMM) or EMM-C (a carbon-depletion version of EMM) for 15 minutes at 30°C. (**B**,**C**) TORC1 activity is inhibited by oxidative and osmotic stresses. JUp1204 (WT) and JUp1350 (*tor2*^{L1310P}) were incubated in EMM containing 1 mM H_2O_2 (B) or 1 M KCl (C) for the indicated time points.

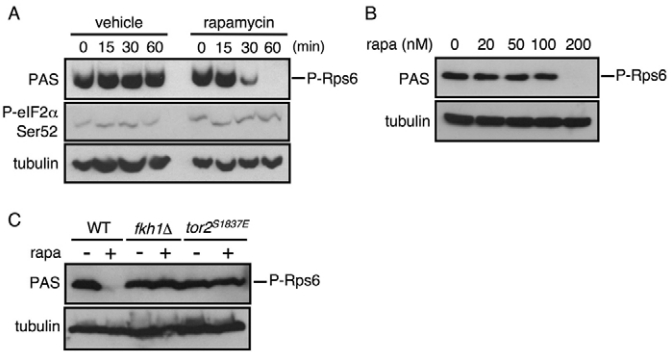

Fig. 7. Rapamycin inhibits Rps6 phosphorylation by blocking TORC1. Extracts were subjected to immunoblotting with the indicated antibodies. (**A**) Cells of JUp1204 (0 minutes) were added with either 200 nM rapamycin or DMSO (vehicle) and incubated for the indicated time points. (**B**) JUp1204 was added with the indicated concentrations of rapamycin (rapa) and incubated for 40 minutes at 30°C. (**C**) Cells of 972 (WT), AN0066 (*fkh1Δ*) and AN0083 (*tor2*^{S1837E}) were added with 200 nM rapamycin and incubated for 40 minutes at 30°C.

results in loss of interaction with the Fkh1-rapamycin complex and suppression of the decreased leucine uptake by rapamycin (Weisman et al., 2005). In the case of *tor2*$^{+}$, the *tor2*^{S1837E} mutation is predicted to confer rapamycin resistance by preventing interaction with the Fkh1-rapamycin complex. Indeed, phosphorylation of Rps6 in the *tor2*^{S1837E} mutant was shown to be completely resistant to rapamycin (Fig. 7C). Similarly, phosphorylation of Rps6 in *fkh1*Δ was not impaired by rapamycin (Fig. 7C). By contrast, Rps6 phosphorylation in the *tor2*^{S1837E} mutant as well as in *fkh1*Δ was abolished under nitrogen-depletion conditions (supplementary material Fig. S5A; data not shown). In addition, Rps6 phosphorylation in the *tor2*^{L1310P} active mutant was sensitive to rapamycin (supplementary material Fig. S5B), similar to the inhibition of the mTOR active mutants by rapamycin in mammalian cells (Urano et al., 2007). These biochemical results suggest that rapamycin inhibits TORC1 activity to regulate Rps6 phosphorylation owing to an interaction of the Fkh1-rapamycin complex with the FRB domain of Tor2.

Rapamycin decreases cell size through Tor2 inhibition

Loss of Tor2 function causes growth defect because of the cell-cycle arrest in G1 phase and promotion of sexual development (Alvarez and Moreno, 2006; Hayashi et al., 2007; Matsuo et al., 2007; Uritani et al., 2006; Weisman et al., 2007). Although rapamycin inhibits TORC1 activity to regulate Rps6 phosphorylation as demonstrated in this study, rapamycin did not interfere with cell proliferation of the wild-type cells as previously reported (data not shown) (Weisman et al., 1997). To further investigate the effect of rapamycin on cell cycle and cell size, we performed flow cytometric analysis to measure DNA content and forward scatter analysis to measure cell size of wild-type and *tor2*^{S1837E} cells after 14 hours incubation in medium with or without rapamycin. Interestingly, the cell size of the wild-type cells was significantly reduced by rapamycin, whereas the reduction by the drug was not observed in *tor2*^{S1837E} (Fig. 8, right panels and bar graph), suggesting that rapamycin decreases cell size via TORC1 inhibition in fission yeast as well as the effect in mammalian cells (Fingar et al., 2002; Kim et al., 2002). Rapamycin did not affect cell cycle in both wild-type or *tor2*^{S1837E} cells (Fig. 8, left panels). By contrast, nitrogen starvation for 14 hours led to accumulation of G1-phase cells (denoted as 1C; Fig. 8, bottom in left panels). Taken together, rapamycin inhibits a subset of the TORC1 functions that are involved in regulation of S6 phosphorylation and cell size but not in cell-cycle progression or cell proliferation.

Discussion

In mammalian cells, the TSC-Rheb-mTORC1 signaling pathway regulates phosphorylation of S6 through activation of S6K in response to several stimuli such as growth factors, nutrients and energy status (Hay and Sonenberg, 2004; Huang and Manning, 2008). We demonstrated here that a similar signal-transduction system is conserved in fission yeast. TORC1 regulates phosphorylation of Rps6 (p27) by sensing nitrogen availability. Phosphorylation of Rps6 in the *tor2* active mutants was maintained at a high level even after the shift to nitrogen depletion. Analogous activating mutations of mTOR confer hyperphosphorylation of S6 when overexpressed in human embryonic kidney (HEK)293 cells starved for nutrients (Urano et al., 2007). Conversely, inactivation of Tor2 in the *tor2-ts* mutants at non-permissive temperature decreased Rps6 phosphorylation in nitrogen-rich conditions. We further showed that TSC-Rhb1 signaling is involved in the TORC1-Rps6 signaling. Downregulation of the TORC1-dependent Rps6 phosphorylation under nitrogen starvation was significantly suppressed either by disruption of *tsc2*$^{+}$, which would cause Rhb1 to be maintained as a GTP-bound form, or by expressing the *rhb1* active mutants.

The Ser235 and Ser236 residues, which are directly phosphorylated by S6K, in S6 are conserved from yeasts to mammal (Ruvinsky and Meyuhas, 2006) (supplementary material Fig. S4). We further demonstrated that these serine residues in Rps6 would be the sites of phosphorylation in response to TORC1 activity. We also indicated that phosphorylation of both the serine residues is dispensable for cell viability in fission yeast. Similarly, in budding yeast, phosphorylation of the conserved serine residues is not necessary for cell survival and protein synthesis (Johnson and Warner, 1987). In the case of mouse, phosphorylation of S6 is also dispensable for cell viability, whereas phosphorylation of the ribosomal protein is involved in cell size and glucose homeostasis (Ruvinsky et al., 2005).

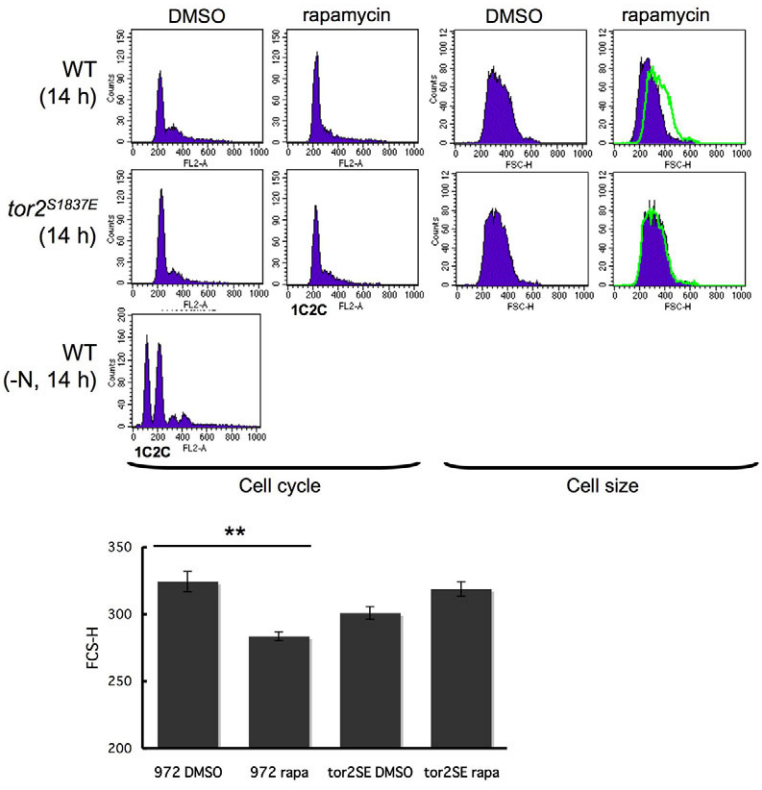

Fig. 8. Rapamycin leads to reduction of cell size in wild-type but not *tor2*^{S1837E} cells. Exponentially growing cells of 972 (WT) and AN0083 (*tor2*^{S1837E}) were diluted to OD_{595}=0.06 and then incubated in EMM with either DMSO (control) or 200 nM rapamycin at 30°C. After 14 hours incubation, the cells were stained with propidium iodide to analyze cellular DNA content and cell size (measured as forward scatter) by flow cytometry. The upper half shows a representative experiment. The green line overlaid on the profile (purple) of cell size from the rapamycin-treated cells indicates the profile outline for control DMSO-treated cells. Profile of DNA content from the wild-type cells that were starved for nitrogen source for 14 hours is shown at the bottom. The bar graph shows the average size as a mean FSC-H ± s.e.m. (n=4). **P<0.01.

Although both alleles of the *tor2-ts* mutants exhibited decreased Rps6 phosphorylation at a non-permissive temperature, there was a difference between the two mutants, *tor2-ts6* and *tor2-ts10*, in the status of Rps6 phosphorylation at a permissive temperature. Whereas Rsp6 phosphorylation in the *tor2-ts6* mutants was abolished under nitrogen starvation, Rps6 phosphorylation in the *tor2-ts10* mutant was maintained even under nitrogen-starvation conditions at a permissive temperature. This particular property of *tor2-ts10* might be due to the fact that the mutant carries two mutations, A1399E in the FAT domain and F2198L in the kinase domain (Matsuo et al., 2007). Therefore, one or both of the mutations in *tor2-ts10* might confer resistance to nitrogen starvation in addition to its temperature sensitivity. In fact, we have found that the *tor2* activating mutations are clustered mainly within or close to the FAT and kinase domains, which are close to the mutation sites in *tor2-ts10* (Urano et al., 2007).

Our demonstration of Rps6 phosphorylation raises the question: what gene encodes S6K? Similar to other eukaryotes, fission yeast has a number of potential AGC kinases, including Sck1, Sck2 and Gad8 (reviewed by Jacinto and Lorberg, 2008). Sck1 and Sck2 are predicted to be homologs of budding yeast SCH9, which has recently been shown to have functional resemblance to S6K (Jacinto and Lorberg, 2008; Urban et al., 2007). In addition, we found by using the BLAST program that another candidate Psk1 has high homology with S6K1. As with other S6K candidates, Psk1 has a conserved hydrophobic motif in which a threonine residue of S6K is directly phosphorylated by mTORC1 in the mammalian system. The mobility shift of these S6K candidates was observed under nitrogen-rich conditions (supplementary material Fig. S6) and phosphatase treatment showed that the mobility shift of the S6K candidates was due to phosphorylation (data not shown). Therefore, phosphorylation of Sck1, Sck2 or Psk1 would be regulated in response to nitrogen availability. These results point to the presence of S6K in fission yeast. Gad8 is a homolog of Akt in mammal and of YPK1 and YPK2 in budding yeast, which are known substrates of TORC2 (Jacinto and Lorberg, 2008; Kamada et al., 2005; Sarbassov et al., 2005), suggesting that Gad8 functions downstream of TORC2. In fact, Gad8 is phosphorylated by TORC2 (Ikeda et al., 2008; Matsuo et al., 2003) and the mobility shift of Gad8 was not affected by nitrogen conditions (supplementary material Fig. S6). By contrast, Hartmuth and Petersen have recently raised the possibility that Gad8 also acts downstream of TORC1, which consists of Tor1 but not of Tor2 (Hartmuth and Petersen, 2009).

TORC1-Rps6 signaling is regulated by glucose status in addition to nitrogen status. In mammalian cells, energy stress caused by glucose depletion activates AMPK. The activated AMPK phosphorylates TSC2 and raptor, thereby inhibiting mTORC1 signaling (reviewed by Dunlop and Tee, 2009; Kimball, 2006). As with Tsc2 and a raptor homolog, Mip1, AMPK homologs exist as Ppk9 and Ssp2 in fission yeast (Hanyu et al., 2009). These AMPKs might act as energy sensors and mediate the energy signaling to TORC1 via phosphorylation of Tsc2 and/or Mip1. Further investigation is needed to gain insights into the regulation of the TORC1-Rps6 signaling by glucose.

We have established that rapamycin inhibits the activity of TORC1 to regulate Rps6 phosphorylation. This inhibition occurred in a manner that the Fkh1-rapamycin complex binds to the FRB domain of Tor2. These results agree with several reports that suggest that rapamycin at least partially inhibits Tor2 functions in fission yeast. Namely, rapamycin prevents proliferation of the *tor1*Δ cells, and this is restored by disruption of *fkh1*$^{+}$ (Kawai et al., 2001; Weisman et al., 2005). A *tor2* temperature-sensitive mutant, *tor2-287* shows growth defect and cell-cycle arrest in G1 phase in the presence of rapamycin (Hayashi et al., 2007). Furthermore, we showed that TORC1 inhibition by rapamycin decreases cell size. Petersen and Nurse have shown that short-term treatment with rapamycin (up to 150 minutes) for synchronized cells promotes mitotic onset that causes the accumulation of small cells (Petersen and Nurse, 2007). In our case, prolonged treatment with rapamycin (14 hours) for asynchronous cells decreases cell size probably without promoting mitotic onset. This is consistent with the observation that rapamycin decreases the size of mammalian cells in an mTORC1-dependent manner (Fingar et al., 2002; Kim et al., 2002).

Unlike the effect of rapamycin on Rps6 phosphorylation and cell size, the drug does not affect cell-cycle progression and cell proliferation. These phenomena by rapamycin are different from those in budding yeast. By contrast, loss of Tor2 function due to temperature-sensitive mutations leads to growth inhibition in fission yeast (Alvarez and Moreno, 2006; Hayashi et al., 2007; Matsuo et al., 2007; Uritani et al., 2006; Weisman et al., 2007). Thus, the rapamycin effects are more limited than the effects of Tor2 inactivation. In addition, decrease in cell size by rapamycin is less dramatic than that caused by the loss of Tor2 function (data not shown). These observations suggest that rapamycin inhibits a subset of TORC1 functions and that rapamycin-resistant function of TORC1 exists. Recently, studies using ATP-competitive mTOR inhibitors in mammalian cells have shown the existence of rapamycin-resistant functions of mTORC1 in the control of cell proliferation, cell size etc. (Feldman et al., 2009; Thoreen et al., 2009). These studies have also shown that mTORC1-S6K-S6 signaling is sensitive to rapamycin, whereas phosphorylations of Thr37 and Thr46 in 4E-BP1 by mTORC1 are resistant. Accordingly, it is probable that fission yeast TORC1 has two different functions: a rapamycin-sensitive function regulating Rps6 phosphorylation and cell size, and a rapamycin-resistant function controlling the switch between cell cycle and cell differentiation, and alteration of gene expression.

Up to now, in fission yeast, alteration of TORC1 activity in *tor2-ts* mutants has been assessed only by the nitrogen-starvation-mimicked cellular responses, including cell-cycle arrest in G1 phase and alteration of gene expression (Alvarez and Moreno, 2006; Hayashi et al., 2007; Matsuo et al., 2007; Urano et al., 2007; Uritani et al., 2006; Weisman et al., 2007). Those cellular responses are not affected by rapamycin (Matsuo et al., 2007; Weisman et al., 1997). Our discovery of S6 in fission yeast provides a new avenue to examine TORC1 activity. Importantly, inactivation of TORC1 occurred rapidly, within 15 minutes after the shift to starvation conditions, and occurred following rapamycin treatment, suggesting that our method enables characterization of early and direct alteration of TORC1 activity during nitrogen starvation. In the mammalian system, a large number of molecules that associate with mTORC1 signaling have been established by assessing function of the molecules in phosphorylation of the TORC1 downstream players such as S6K1, 4E-BP1 and S6. In the future, assessment of Rps6 phosphorylation will be useful in studying the molecules that associate with the TORC1 signaling in fission yeast.

Materials and Methods

Yeast strains, growth media and general methods

The fission yeast strains used in this study are listed in supplementary material Table S1. Cells were grown in yeast extract with supplements (YES) medium or Edinburgh minimal medium (EMM) supplemented with 200 mg/l adenine, when necessary, which contains 2% glucose as a carbon source and 0.5% ammonium chloride as a nitrogen source (Moreno et al., 1991). EMM-N, a nitrogen-free version, and EMM-C (3% glycerol and 0.1% glucose), a carbon-depletion version, were employed as starvation

media (Kohda et al., 2007). General and molecular genetic techniques followed standard protocols (Moreno et al., 1991). Transformation was performed by the lithium-acetate method (Okazaki et al., 1990).

Antibodies and reagents

Anti-PAS and anti-phospho-eIF2α (Ser51) polyclonal antibodies were purchased from Cell Signaling Technology. Anti-FLAG (M2) and anti-α-tubulin (B5-1-2) antibodies were purchased from Sigma. Anti-Myc (9E10) antibody was purchased from Santa Cruz Biotechnology. Horseradish peroxidase (HRP)-conjugated goat anti-mouse IgG antibody and protein-G–Sepharose were purchased from GE Healthcare Bio-Sciences. HRP-conjugated donkey anti-rabbit IgG antibody and HRP-conjugated protein A were purchased from Pierce and Invitrogen, respectively. Rapamycin was purchased from Calbiochem.

Gene disruption and construction of mutant strains and the gene expression plasmids

Disruption of *rps601*$^+$ or *rps602*$^+$ genes was performed using the direct chromosomal integration method as described previously (Bahler et al., 1998; Sato et al., 2005). The entire open reading frames (ORFs) of *rps601*$^+$ and *rps602*$^+$ were substituted by the *kanMX* or *hphMX* cassette. The 3×HA-*hphMX* or 13×myc-*hphMX* cassette was integrated into the C-terminus of *sck1*$^+$, *sck2*$^+$, *gad8*$^+$ or *psk1*$^+$ via the similar PCR-base method. To construct a *myc-rps602*$^+$ allele that expresses an N-terminal tagged myc-*rps602*$^+$ under the control of its own promoter, the *myc-rps602NT* DNA fragment (880 bp) including 470 bp of 5′ UTR region of *rps602*$^+$ and one copy of the myc epitope tag before the start codon of *rps602*$^+$ were introduced by two-step PCR using genomic DNA as the template and cloned to generate the pUG6-*myc-rps602NT* plasmid. The DNA fragment containing the *myc-rps602NT* and the *kanMX* cassette was inserted by homologous recombination after digesting the plasmid with a restriction enzyme (*Age*I). To construct the *rps602*^{S235A,S236A} allele that expresses, under the control of its own promoter, the C-terminal *rps602SSAA* DNA fragment (718 bp), including mutations of *rps602*^{S235A,S236A} and 370 bp of its 3′ UTR was amplified by two-step PCR using genomic DNA as the template and cloned to generate the pUG6-*rps602SSAACT* plasmid. pUG6-*rps602SSAACT* was inserted by homologous recombination after digesting the plasmid with *Blp*I. To construct the *tor2*^{S1837E} mutant, the mutation was generated by site-directed mutagenesis using pUG6-*tor2*-CTL (Urano et al., 2007) and the sequence was confirmed. The pUG6-*tor2*^{S1837E}-CTL plasmid was inserted by homologous recombination as described previously (Urano et al., 2007).

For construction of a series of the expression plasmids of *rps601*$^+$ or *rps602*$^+$, we first created a pREP1-myc vector in which the NTAP tag in pREP1-NTAP (Tasto et al., 2001) is replaced with one copy of the myc-epitope tag. The *rps601*$^+$ and *rps602*$^+$ ORFs were amplified by PCR and cloned behind the myc-epitope tag by using *Nde*I and *Bam*HI. The substitution of Ser235 and/or Ser236 with Ala in *rps601*$^+$ or *rps602*$^+$ was performed by PCR amplification using the series of primers that contained those substitutions. pRPL-myc-*rhb1*^{S16H} was generated by site-directed mutagenesis using the pRPL-myc-*rhb1*$^+$ plasmid (Urano et al., 2007) as a template. pREP41-His6FLAG2-*tor2*$^+$ and pREP41-His6FLAG2-*tor2*^{E2221K} were generated as described previously (Matsuo et al., 2007; Urano et al., 2007).

Protein preparation and immunoprecipitation

For detecting phosphoproteins, harvested cells were boiled for 5 minutes and disrupted with glass beads in buffer A [50 mM Tris-HCl (pH 7.5), 150 mM NaCl, 5 mM EDTA, 10% glycerol, 0.2% NP-40, 20 mM β-glycerophosphate, 0.1 mM Na_3VO_4, 10 mM p-nitrophenyl phosphate (p-NPP), 10 mM NaF, 1 mM dithiothreitol (DTT), 1 mM phenylmethylsulfonyl fluoride (PMSF), and protease inhibitor cocktail (Complete EDTA-free; Roche)]. The whole-cell extracts were added with 3× SDS sample buffer and then boiled for 5 minutes. The samples were separated by SDS-PAGE and subjected to immunoblotting using each primary antibody. Detection of the proteins was carried out using ECL plus detection system (GE Healthcare Bio-Sciences).

For phosphatase treatment, harvested cells were disrupted with glass beads in buffer A. The cell extracts were diluted with λ-phosphatase reaction buffer and 2 mM $MnCl_2$, and then incubated with λ-phosphatase (New England Biolabs) at 30°C for 40 minutes either with or without the phosphatase inhibitors (50 mM EDTA, 10 mM Na_3VO_4 and 50 mM NaF).

To immunoprecipitate myc-tagged Rps6, harvested cells were disrupted with glass beads in buffer B [50 mM Tris-HCl (pH 7.5), 200 mM NaCl, 5 mM EDTA, 10% glycerol, 0.2% NP-40, 20 mM β-glycerophosphate, 1 mM Na_3VO_4, 10 mM p-NPP, 10 mM NaF, 1 mM DTT, 1 mM PMSF, 20 μg/ml leupeptin, 10 μg/ml pepstatin A, and protease inhibitor cocktail]. Glass beads and cell debris were removed by the centrifugation at 10,000 ***g*** for 15 minutes at 4°C. In total, 10 mg of proteins from the centrifugation at 14,000 ***g*** for 20 minutes at 4°C was incubated with anti-myc (9E10) antibody and protein-G–Sepharose beads at 4°C for 1.5 hours. Immunoprecipitates were washed three times with buffer B without protease inhibitors. To detect phosphorylation of the immunoprecipitated myc-tagged Rps6, HRP-conjugated protein A was employed instead of the HRP-conjugated anti-rabbit antibody.

Cell-cycle and cell-size analysis

Cells were fixed in 70% cold ethanol and stained with propidium iodide for FACS analysis (cell cycle) and forward scatter analysis (cell size) as described previously (Urano et al., 2007). Four independent experiments were repeated and, in each experiment, more than 1.2×10^4 cell events were measured.

We thank other members of our lab for helpful discussions and for technical assistance, and Masayuki Yamamoto, Susan Forsburg, Ronit Weisman and National BioResource Project (NBRP) for providing yeast strains. This work was supported by NIH grant CA41996. Deposited in PMC for release after 12 months.

Supplementary material available online at
http://jcs.biologists.org/cgi/content/full/123/5/777/DC1

References

Alvarez, B. and Moreno, S. (2006). Fission yeast Tor2 promotes cell growth and represses cell differentiation. *J. Cell Sci*. **119**, 4475-4485.

Aspuria, P. J. and Tamanoi, F. (2008). The Tsc/Rheb signaling pathway controls basic amino acid uptake via the Cat1 permease in fission yeast. *Mol. Genet. Genomics* **279**, 441-450.

Aspuria, P. J., Sato, T. and Tamanoi, F. (2007). The TSC/Rheb/TOR signaling pathway in fission yeast and mammalian cells: temperature sensitive and constitutive active mutants of TOR. *Cell Cycle* **6**, 1692-1695.

Bahler, J., Wu, J. Q., Longtine, M. S., Shah, N. G., McKenzie, A., III, Steever, A. B., Wach, A., Philippsen, P. and Pringle, J. R. (1998). Heterologous modules for efficient and versatile PCR-based gene targeting in *Schizosaccharomyces pombe*. *Yeast* **14**, 943-951.

Bonnet, C., Perret, E., Dumont, X., Picard, A., Caput, D. and Lenaers, G. (2000). Identification and transcription control of fission yeast genes repressed by an ammonium starvation growth arrest. *Yeast* **16**, 23-33.

Chen, J., Zheng, X. F., Brown, E. J. and Schreiber, S. L. (1995). Identification of an 11-kDa FKBP12-rapamycin-binding domain within the 289-kDa FKBP12-rapamycin-associated protein and characterization of a critical serine residue. *Proc. Natl. Acad. Sci. USA* **92**, 4947-4951.

Cherkasova, V. A. and Hinnebusch, A. G. (2003). Translational control by TOR and TAP42 through dephosphorylation of eIF2alpha kinase GCN2. *Genes Dev*. **17**, 859-872.

Chiang, G. G. and Abraham, R. T. (2007). Targeting the mTOR signaling network in cancer. *Trends Mol. Med.* **13**, 433-442.

Dunlop, E. A. and Tee, A. R. (2009). Mammalian target of rapamycin complex **1**, signalling inputs, substrates and feedback mechanisms. *Cell. Signal*. **21**, 827-835.

Eguchi, S., Oshiro, N., Miyamoto, T., Yoshino, K., Okamoto, S., Ono, T., Kikkawa, U. and Yonezawa, K. (2009). AMP-activated protein kinase phosphorylates glutamine: fructose-6-phosphate amidotransferase 1 at Ser243 to modulate its enzymatic activity. *Genes Cells* **14**, 179-189.

Feldman, M. E., Apsel, B., Uotila, A., Loewith, R., Knight, Z. A., Ruggero, D. and Shokat, K. M. (2009). Active-site inhibitors of mTOR target rapamycin-resistant outputs of mTORC1 and mTORC2. *PLoS Biol*. **7**, e38.

Fingar, D. C., Salama, S., Tsou, C., Harlow, E. and Blenis, J. (2002). Mammalian cell size is controlled by mTOR and its downstream targets S6K1 and 4EBP1/eIF4E. *Genes Dev*. **16**, 1472-1487.

Gao, X., Zhang, Y., Arrazola, P., Hino, O., Kobayashi, T., Yeung, R. S., Ru, B. and Pan, D. (2002). Tsc tumour suppressor proteins antagonize amino-acid-TOR signalling. *Nat. Cell Biol.* **4**, 699-704.

Garami, A., Zwartkruis, F. J., Nobukuni, T., Joaquin, M., Roccio, M., Stocker, H., Kozma, S. C., Hafen, E., Bos, J. L. and Thomas, G. (2003). Insulin activation of Rheb, a mediator of mTOR/S6K/4E-BP signaling, is inhibited by TSC1 and 2. *Mol. Cell* **11**, 1457-1466.

Hanyu, Y., Imai, K. K., Kawasaki, Y., Nakamura, T., Nakaseko, Y., Nagao, K., Kokubu, A., Ebe, M., Fujisawa, A., Hayashi, T. et al. (2009). *Schizosaccharomyces pombe* cell division cycle under limited glucose requires Ssp1 kinase, the putative CaMKK, and Sds23, a PP2A-related phosphatase inhibitor. *Genes Cells* **14**, 539-554.

Hartmuth, S. and Petersen, J. (2009). Fission yeast Tor1 functions as part of TORC1 to control mitotic entry through the stress MAPK pathway following nutrient stress. *J. Cell Sci.* **122**, 1737-1746.

Hay, N. and Sonenberg, N. (2004). Upstream and downstream of mTOR. *Genes Dev*. **18**, 1926-1945.

Hayashi, T., Hatanaka, M., Nagao, K., Nakaseko, Y., Kanoh, J., Kokubu, A., Ebe, M. and Yanagida, M. (2007). Rapamycin sensitivity of the *Schizosaccharomyces pombe* tor2 mutant and organization of two highly phosphorylated TOR complexes by specific and common subunits. *Genes Cells* **12**, 1357-1370.

Helliwell, S. B., Wagner, P., Kunz, J., Deuter-Reinhard, M., Henriquez, R. and Hall, M. N. (1994). TOR1 and TOR2 are structurally and functionally similar but not identical phosphatidylinositol kinase homologues in yeast. *Mol. Biol. Cell* **5**, 105-118.

Hidayat, S., Yoshino, K., Tokunaga, C., Hara, K., Matsuo, M. and Yonezawa, K. (2003). Inhibition of amino acid-mTOR signaling by a leucine derivative induces G1 arrest in Jurkat cells. *Biochem. Biophys. Res. Commun.* **301**, 417-423.

Hilti, N., Baumann, D., Schweingruber, A. M., Bigler, P. and Schweingruber, M. E. (1999). Gene *ste20* controls amiloride sensitivity and fertility in *Schizosaccharomyces pombe*. *Curr. Genet*. **35**, 585-592.

Huang, J. and Manning, B. D. (2008). The TSC1-TSC2 complex: a molecular switchboard controlling cell growth. *Biochem. J.* **412**, 179-190.
Ikeda, K., Morigasaki, S., Tatebe, H., Tamanoi, F. and Shiozaki, K. (2008). Fission yeast TOR complex 2 activates the AGC-family Gad8 kinase essential for stress resistance and cell cycle control. *Cell Cycle* **7**, 358-364.
Inoki, K., Li, Y., Zhu, T., Wu, J. and Guan, K. L. (2002). TSC2 is phosphorylated and inhibited by Akt and suppresses mTOR signalling. *Nat. Cell Biol.* **4**, 648-657.
Jacinto, E. and Lorberg, A. (2008). TOR regulation of AGC kinases in yeast and mammals. *Biochem. J.* **410**, 19-37.
Johnson, S. P. and Warner, J. R. (1987). Phosphorylation of the *Saccharomyces cerevisiae* equivalent of ribosomal protein S6 has no detectable effect on growth. *Mol. Cell. Biol.* **7**, 1338-1345.
Kamada, Y., Fujioka, Y., Suzuki, N. N., Inagaki, F., Wullschleger, S., Loewith, R., Hall, M. N. and Ohsumi, Y. (2005). Tor2 directly phosphorylates the AGC kinase Ypk2 to regulate actin polarization. *Mol. Cell. Biol.* **25**, 7239-7248.
Kane, S., Sano, H., Liu, S. C., Asara, J. M., Lane, W. S., Garner, C. C. and Lienhard, G. E. (2002). A method to identify serine kinase substrates. Akt phosphorylates a novel adipocyte protein with a Rab GTPase-activating protein (GAP) domain. *J. Biol. Chem.* **277**, 22115-22118.
Kato, T., Jr, Okazaki, K., Murakami, H., Stettler, S., Fantes, P. A. and Okayama, H. (1996). Stress signal, mediated by a Hog1-like MAP kinase, controls sexual development in fission yeast. *FEBS Lett.* **378**, 207-212.
Kawai, M., Nakashima, A., Ueno, M., Ushimaru, T., Aiba, K., Doi, H. and Uritani, M. (2001). Fission yeast tor1 functions in response to various stresses including nitrogen starvation, high osmolarity, and high temperature. *Curr. Genet.* **39**, 166-174.
Kim, D. H., Sarbassov, D. D., Ali, S. M., King, J. E., Latek, R. R., Erdjument-Bromage, H., Tempst, P. and Sabatini, D. M. (2002). mTOR interacts with raptor to form a nutrient-sensitive complex that signals to the cell growth machinery. *Cell* **110**, 163-175.
Kimball, S. R. (2006). Interaction between the AMP-activated protein kinase and mTOR signaling pathways. *Med. Sci. Sports Exerc.* **38**, 1958-1964.
Kohda, T. A., Tanaka, K., Konomi, M., Sato, M., Osumi, M. and Yamamoto, M. (2007). Fission yeast autophagy induced by nitrogen starvation generates a nitrogen source that drives adaptation processes. *Genes Cells* **12**, 155-170.
Kubota, H., Obata, T., Ota, K., Sasaki, T. and Ito, T. (2003). Rapamycin-induced translational derepression of GCN4 mRNA involves a novel mechanism for activation of the eIF2 alpha kinase GCN2. *J. Biol. Chem.* **278**, 20457-20460.
Kunitomo, H., Higuchi, T., Iino, Y. and Yamamoto, M. (2000). A zincfinger protein, Rst2p, regulates transcription of the fission yeast *ste11*$^{+}$ gene, which encodes a pivotal transcription factor for sexual development. *Mol. Biol. Cell* **11**, 3205-3217.
Lorenz, M. C. and Heitman, J. (1995). TOR mutations confer rapamycin resistance by preventing interaction with FKBP12-rapamycin. *J. Biol. Chem.* **270**, 27531-27537.
Mach, K. E., Furge, K. A. and Albright, C. F. (2000). Loss of Rhb1, a Rheb-related GTPase in fission yeast, causes growth arrest with a terminal phenotype similar to that caused by nitrogen starvation. *Genetics* **155**, 611-622.
Manning, B. D., Tee, A. R., Logsdon, M. N., Blenis, J. and Cantley, L. C. (2002). Identification of the tuberous sclerosis complex-2 tumor suppressor gene product tuberin as a target of the phosphoinositide 3-kinase/akt pathway. *Mol. Cell* **10**, 151-162.
Matsumoto, S., Bandyopadhyay, A., Kwiatkowski, D. J., Maitra, U. and Matsumoto, T. (2002). Role of the Tsc1-Tsc2 complex in signaling and transport across the cell membrane in the fission yeast *Schizosaccharomyces pombe*. *Genetics* **161**, 1053-1063.
Matsuo, T., Kubo, Y., Watanabe, Y. and Yamamoto, M. (2003). *Schizosaccharomyces pombe* AGC family kinase Gad8p forms a conserved signaling module with TOR and PDK1-like kinases. *EMBO J.* **22**, 3073-3083.
Matsuo, T., Otsubo, Y., Urano, J., Tamanoi, F. and Yamamoto, M. (2007). Loss of the TOR kinase Tor2 mimics nitrogen starvation and activates the sexual development pathway in fission yeast. *Mol. Cell. Biol.* **27**, 3154-3164.
Miyamoto, T., Oshiro, N., Yoshino, K., Nakashima, A., Eguchi, S., Takahashi, M., Ono, Y., Kikkawa, U. and Yonezawa, K. (2008). AMP-activated protein kinase phosphorylates Golgi-specific brefeldin A resistance factor 1 at Thr1337 to induce disassembly of Golgi apparatus. *J. Biol. Chem.* **283**, 4430-4438.
Moreno, S., Klar, A. and Nurse, P. (1991). Molecular genetic analysis of fission yeast *Schizosaccharomyces pombe*. *Methods Enzymol.* **194**, 795-823.
Murai, T., Nakase, Y., Fukuda, K., Chikashige, Y., Tsutsumi, C., Hiraoka, Y. and Matsumoto, T. (2009). Distinctive responses to nitrogen starvation in the dominant active mutants of the fission yeast Rheb GTPase. *Genetics* **183**, 517-527.
Nakase, Y., Fukuda, K., Chikashige, Y., Tsutsumi, C., Morita, D., Kawamoto, S., Ohnuki, M., Hiraoka, Y. and Matsumoto, T. (2006). A defect in protein farnesylation suppresses a loss of *Schizosaccharomyces pombe tsc2*$^{+}$, a homolog of the human gene predisposing to tuberous sclerosis complex. *Genetics* **173**, 569-578.
Nakashima, A., Yoshida, M., Nakayama, K., Kato-Furuno, A., Ueno, M., Ushimaru, T. and Uritani, M. (2002). Genes for a nuclease and a protease are involved in the drastic decrease in cellular RNA amount in fission yeast cells during nitrogen starvation. *J. Biochem.* **131**, 391-398.
Okazaki, K., Okazaki, N., Kume, K., Jinno, S., Tanaka, K. and Okayama, H. (1990). High-frequency transformation method and library transducing vectors for cloning mammalian cDNAs by transcomplementation of *Schizosaccharomyces pombe*. *Nucleic Acids Res.* **18**, 6485-6489.
Otsubo, Y. and Yamamato, M. (2008). TOR signaling in fission yeast. *Crit. Rev. Biochem. Mol. Biol.* **43**, 277-283.
Patel, J., McLeod, L. E., Vries, R. G., Flynn, A., Wang, X. and Proud, C. G. (2002). Cellular stresses profoundly inhibit protein synthesis and modulate the states of phosphorylation of multiple translation factors. *Eur. J. Biochem.* **269**, 3076-3085.
Petersen, J. and Nurse, P. (2007). TOR signalling regulates mitotic commitment through the stress MAP kinase pathway and the Polo and Cdc2 kinases. *Nat. Cell Biol.* **9**, 1263-1272.
Ruvinsky, I. and Meyuhas, O. (2006). Ribosomal protein S6 phosphorylation: from protein synthesis to cell size. *Trends Biochem. Sci.* **31**, 342-348.
Ruvinsky, I., Sharon, N., Lerer, T., Cohen, H., Stolovich-Rain, M., Nir, T., Dor, Y., Zisman, P. and Meyuhas, O. (2005). Ribosomal protein S6 phosphorylation is a determinant of cell size and glucose homeostasis. *Genes Dev.* **19**, 2199-2211.
Sarbassov, D. D., Guertin, D. A., Ali, S. M. and Sabatini, D. M. (2005). Phosphorylation and regulation of Akt/PKB by the rictor-mTOR complex. *Science* **307**, 1098-1101.
Sato, M., Dhut, S. and Toda, T. (2005). New drug-resistant cassettes for gene disruption and epitope tagging in *Schizosaccharomyces pombe*. *Yeast* **22**, 583-591.
Shiozaki, K. and Russell, P. (1996). Conjugation, meiosis, and the osmotic stress response are regulated by Spc1 kinase through Atf1 transcription factor in fission yeast. *Genes Dev.* **10**, 2276-2288.
Stan, R., McLaughlin, M. M., Cafferkey, R., Johnson, R. K., Rosenberg, M. and Livi, G. P. (1994). Interaction between FKBP12-rapamycin and TOR involves a conserved serine residue. *J. Biol. Chem.* **269**, 32027-32030.
Tabancay, A. P., Jr, Gau, C. L., Machado, I. M., Uhlmann, E. J., Gutmann, D. H., Guo, L. and Tamanoi, F. (2003). Identification of dominant negative mutants of Rheb GTPase and their use to implicate the involvement of human Rheb in the activation of p70S6K. *J. Biol. Chem.* **278**, 39921-39930.
Tasto, J. J., Carnahan, R. H., McDonald, W. H. and Gould, K. L. (2001). Vectors and gene targeting modules for tandem affinity purification in *Schizosaccharomyces pombe*. *Yeast* **18**, 657-662.
Tee, A. R., Manning, B. D., Roux, P. P., Cantley, L. C. and Blenis, J. (2003). Tuberous sclerosis complex gene products, Tuberin and Hamartin, control mTOR signaling by acting as a GTPase-activating protein complex toward Rheb. *Curr. Biol.* **13**, 1259-1268.
Thoreen, C. C., Kang, S. A., Chang, J. W., Liu, Q., Zhang, J., Gao, Y., Reichling, L. J., Sim, T., Sabatini, D. M. and Gray, N. S. (2009). An ATP-competitive mammalian target of rapamycin inhibitor reveals rapamycin-resistant functions of mTORC1. *J. Biol. Chem.* **284**, 8023-8032.
Urano, J., Comiso, M. J., Guo, L., Aspuria, P. J., Deniskin, R., Tabancay, A. P., Jr, Kato-Stankiewicz, J. and Tamanoi, F. (2005). Identification of novel single amino acid changes that result in hyperactivation of the unique GTPase, Rheb, in fission yeast. *Mol. Microbiol.* **58**, 1074-1086.
Urano, J., Sato, T., Matsuo, T., Otsubo, Y., Yamamoto, M. and Tamanoi, F. (2007). Point mutations in TOR confer Rheb-independent growth in fission yeast and nutrient-independent mammalian TOR signaling in mammalian cells. *Proc. Natl. Acad. Sci. USA* **104**, 3514-3519.
Urban, J., Soulard, A., Huber, A., Lippman, S., Mukhopadhyay, D., Deloche, O., Wanke, V., Anrather, D., Ammerer, G., Riezman, H. et al. (2007). Sch9 is a major target of TORC1 in *Saccharomyces cerevisiae*. *Mol. Cell* **26**, 663-674.
Uritani, M., Hidaka, H., Hotta, Y., Ueno, M., Ushimaru, T. and Toda, T. (2006). Fission yeast Tor2 links nitrogen signals to cell proliferation and acts downstream of the Rheb GTPase. *Genes Cells* **11**, 1367-1379.
van Slegtenhorst, M., Carr, E., Stoyanova, R., Kruger, W. D. and Henske, E. P. (2004). *tsc1*$^{+}$ and *tsc2*$^{+}$ regulate arginine uptake and metabolism in *Schizosaccharomyces pombe*. *J. Biol. Chem.* **279**, 12706-12713.
Weisman, R. and Choder, M. (2001). The fission yeast TOR homolog, *tor1*$^{+}$, is required for the response to starvation and other stresses via a conserved serine. *J. Biol. Chem.* **276**, 7027-7032.
Weisman, R., Choder, M. and Koltin, Y. (1997). Rapamycin specifically interferes with the developmental response of fission yeast to starvation. *J. Bacteriol.* **179**, 6325-6334.
Weisman, R., Roitburg, I., Nahari, T. and Kupiec, M. (2005). Regulation of leucine uptake by *tor1*$^{+}$ *in Schizosaccharomyces pombe* is sensitive to rapamycin. *Genetics* **16**, 539-550.
Weisman, R., Roitburg, I., Schonbrun, M., Harari, R. and Kupiec, M. (2007). Opposite effects of Tor1 and Tor2 on nitrogen starvation responses in fission yeast. *Genetics* **175**, 1153-1162.
Wilkinson, M. G., Samuels, M., Takeda, T., Toone, W. M., Shieh, J. C., Toda, T., Millar, J. B. and Jones, N. (1996). The Atf1 transcription factor is a target for the Sty1 stress-activated MAP kinase pathway in fission yeast. *Genes Dev.* **10**, 2289-2301.
Wullschleger, S., Loewith, R. and Hall, M. N. (2006). TOR signaling in growth and metabolism. *Cell* **124**, 471-484.
Yaffe, M. B., Leparc, G. G., Lai, J., Obata, T., Volinia, S. and Cantley, L. C. (2001). A motif-based profile scanning approach for genome-wide prediction of signaling pathways. *Nat. Biotechnol.* **19**, 348-353.
Yan, L., Findlay, G. M., Jones, R., Procter, J., Cao, Y. and Lamb, R. F. (2006). Hyperactivation of mammalian target of rapamycin (mTOR) signaling by a gain-of-function mutant of the Rheb GTPase. *J. Biol. Chem.* **281**, 19793-19797.
Yang, W., Tabancay, A. P., Jr, Urano, J. and Tamanoi, F. (2001). Failure to farnesylate Rheb protein contributes to the enrichment of G0/G1 phase cells in the *Schizosaccharomyces pombe* farnesyltransferase mutant. *Mol. Microbiol.* **41**, 339-347.
Zhan, K., Narasimhan, J. and Wek, R. C. (2004). Differential Activation of eIF2 Kinases in Response to Cellular Stresses in *Schizosaccharomyces pombe*. *Genetics* **168**, 1867-1875.

Table S1. Fission yeast strains used in this study

Strain	Genotype	Reference/source
972	*h⁻*	Lab stock
JY450	*h⁹⁰ ade6-M216 leu1-32*	M. Yamamoto
JT293	*h⁹⁰ ade6-M216 leu1 ura4-D18 ste20::ura4⁺*	Matsuo et al., 2007
JZ858	*h⁹⁰ ade6-M216 leu1 ura4-D18 cgs1::ura4⁺*	Kunitomo et al., 2000
TA99	*h⁻ ade6-M216 leu1-32 ura4-D18 tor1::ura4⁺*	Weisman and Choder, 2001
FY13927	*h⁹⁰ leu1 ura4-D18 phh1::ura4⁺*	National-Bio-Resource-Project
PJ001	*h⁻ tsc2::kanMX*	Aspuria and Tamanoi, 2008
JUp1188	*mycRhb1⁺*	Lab stock
JUp1190	*mycRhb1^{V17A}*	Lab stock
JUp1194	*mycRhb1^{K120R}*	Lab stock
JUp1204	*h⁹⁰ FY155*	S. Forsburg
JUp1209	*h⁹⁰ leu1-32 ura4-D18*	Lab stock
JUp1210	*h⁹⁰ ura4-D18*	Lab stock
JUp1211	*h⁹⁰ leu1-32*	Lab stock
JUp1246	*h⁹⁰*	Lab stock
JUp1247	*h⁹⁰ tor2-ts6*	Lab stock Matsuo et al., 2007
JUp1252	*h⁹⁰ tor2-ts10*	Lab stock Matsuo et al., 2007
JUp1348	*h⁹⁰ tor2⁺:kanMX*	Urano et al., 2007
JUp1350	*h⁹⁰ tor2^{L1310P}:kanMX*	Urano et al., 2007
JUp1352	*h⁹⁰ tor2^{E2221K}:kanMX*	Urano et al., 2007
AN0066	*h⁻ fkh1::ura4⁺*	This study, Weisman et al., 2005
AN0083	*h⁻ tor2^{S1837E}:kanMX*	This study
AN0094	*h⁻ rps601::hphMX*	This study
AN0097	*h⁻ rps602::hphMX*	This study
AN0098	*h⁹⁰ rps602::kanMX leu1-32*	This study
AN0129	*h⁹⁰ rps601::hphMX kanMX:rps602-pro-myc-rps602⁺*	This study
AN0228	*h⁻ rps601::hphMX rps602SS235236AA:kanMX #1*	This study
AN0229	*h⁻ rps601::hphMX rps602SS235236AA:kanMX #2*	This study